Semi-annual report of work progress on NASA grant NASW-4933

"Plasma Properties and Magnetic Field Structure of the Solar Corona, Based on Coordinated Max '91 Observations from SERTS, the VLA, and Magnetographs"

covering the period 12 July 1995 — 11 January 1996

PRINCIPAL INVESTIGATOR:

Dr. Jeffrey W. Brosius
Hughes STX Corporation
4400 Forbes Boulevard
Lanham, MD 20706-4392
Tel.: (301) 286-6200

1 Introduction

The purposes of this investigation are to determine the plasma properties and magnetic field structure of the solar corona using coordinated observations obtained with NASA/GSFC's Solar EUV Rocket Telescope and Spectrograph (SERTS), the Very Large Array (VLA), and magnetographs. The observations were obtained under the auspices of NASA's Max '91 program. The methods of achieving the stated purposes are to use SERTS spectra and spectroheliograms to determine coronal plasma properties such as temperature, density, and emission measure. These properties are subsequently used to calculate the intensity of the thermal bremsstrahlung microwave emission from the coronal plasma (the minimum microwave intensity expected from the emitting plasma). This, in turn, can be used to establish which emission mechanism(s) contribute to the observed microwave emission. Because both mechanisms that may contribute to quiescent active region microwave emission (thermal bremsstrahlung and thermal gyroemission) depend upon the coronal magnetic field in known ways, this information can ultimately be used to derive the coronal magnetic field. Ideally, three-dimensional models of the coronal plasma and magnetic field which are consistent with all of the EUV spectra and spectroheliograms, as well as with the intensity and polarization maps at all of the microwave observing frequencies, can be derived. For completeness, the coronal magnetic field derived from the coordinated multiwaveband observations must be compared with extrapolations from photospheric magnetograms.

2 Achievements

Oxymoronic though it may sound, unexpected difficulties were anticipated for this project. One such major difficulty, concerning the SERTS calibration measured in the laboratory, has raised currently unanswered questions concerning the calibration of multilayer coated diffraction gratings. Before I became involved in this project, GSFC personnel obtained laboratory calibration curves separately for each of the three optical components of the SERTS instrument: an aluminum filter, a grazing incidence telescope, and a multilayer coated diffraction grating. The calibration curves of the first two components are slowly varying and nearly offsetting (so that the net curve is fairly flat). The curve for the multilayer coated diffraction grating was designed to have a high, somewhat broad peak around 300 Å. The curve measured in the laboratory, during two separate observing runs at NIST's SURF-II facility (Thomas, Keski-Kuha, Neupert, Condor, & Gum 1991, Appl. Opt., 30, 2245; repeated in July 1995), yielded good agreement with the design curve. The measurements were clean and reproducible. I adopted those measurements for this project, and believed that I had well calibrated data as a starting point.

When the measured calibration curve was applied to solar observations obtained during the SERTS flights of 1991 May 7 and 1993 August 17, some of the measured density- and temperature-insensitive line intensity ratios disagreed with their corresponding theoretical values by factors as high as 10. This was disturbing, but was originally attributed to errors in the measured calibration for lines shortward of 300 Å. All available ratios among lines longward of 300 Å agreed with their corresponding theoretical values reasonable well, typically within the measured error bars. (Initially, all ratio pairs involved two lines in the range 300 to 322 Å, or two lines in the range 327 to 417 Å. All such ratios agreed well with their theoretical values.) However, several factors eventually indicated that the calibration problem was more widespread than originally believed. First, many

of the density-sensitive line intensity ratios involving one line longward of 325 Å and one line shortward of 325 Å were either much higher or much lower than their corresponding theoretical ranges. Second, a previously unidentified Fe XIII line at 312.9 Å was identified, and found to be a member of a density- and temperature-insensitive pair (the other line being that of Fe XIII at 359.7 Å). The measured ratio disagreed with its theoretical value. Third, new atomic physics calculations for Mg VIII were kindly provided by Dr. Anand K. Bhatia, and further indicated that a relative calibration problem existed between lines shortward of 325 Å and those longward of 325 Å. Thus it became apparent that the measured calibration curve, despite its cleanliness and its reproducibility, simply did not make sense in light of measured line intensity ratios.

Once the calibration problem was identified, it was corrected by deriving a modified calibration curve such that all available density- and temperature-insensitive line intensity ratios of Fe X, Fe XI, Fe XII, Fe XIII, Fe XIV, Fe XV, Fe XVI, Si VIII, Si IX, Mg VIII, and Ni XVIII in the wavelength range from 274 to 420 Å agree with their appropriate theoretical values. This yields a region of sensitivity enhancement for the multilayer coated diffraction grating that is narrower than measured in the laboratory. Explanations for the discrepancy are not currently known. Since the purpose of this project is to derive coronal plasma properties and magnetic fields, and not to characterize the response of the SERTS instrument, I will pursue the subject no further under this grant.

It should be pointed out that the theoretical line intensity ratios for iron and silicon are all derived from line emissivity tables provided by Dr. Brunella Monsignori-Fossi. These tables were revised during summer 1995, and so the updated versions of all those tables were incorporated in the SERTS calibration revision as well as in the temperature and density diagnostics. In addition, I used very recent calculations for Mg VIII, completed and kindly provided by Dr. Anand K. Bhatia.

After the revised calibration curve was obtained, new emission line tables were obtained for each of the five averaged spectra which were obtained from the 1991 and the 1993 SERTS flights. In addition, the range of wavelength coverage was extended from 300 down to 274 Å, so that up to seven additional emission lines became available for diagnostics. For the 1991 flight, I have an active region, quiet sun, and off-limb averaged spectrum, and for the 1993 flight I have an active region and a quiet sun averaged spectrum. Table 1 lists the available density- and temperature-insensitive line intensity ratios. Figure 1 shows the ratios of the measured to the theoretical ratios, only for the 1993 flight, plotted as a function of wavelength. Each ratio of ratios appears twice, once at each wavelength in the pair. Some scatter (typically less than a factor of 2) is evident, but no systematic trend is visible.

Line-ratio densities and temperatures were re-derived using the revised list of line intensities. Densities are listed in Table 2 and plotted in Figure 2; temperatures are listed in Table 4. With the densities, intensities, and emissivities, filling factors were derived. These are listed in Table 3.

The IDL code for calculating the microwave emission from a plasma with specified magnetic field structure was revised, and additional necessary changes were identified. In particular, the code needs to be modified in order to better handle the steep gradients in optical depth associated with gyroresonance emission.

The Kitt Peak photospheric longitudinal magnetogram was precisely coaligned with the SERTS images and with the He I 10830 image. (Despite the fact that the He I 10830 and the photospheric

longitudinal magnetogram both come from Kitt Peak, their coalignment is neither automatic nor trivial.)

The VLA microwave intensity (I) and Stokes V maps were crudely coaligned and qualitatively compared with the SERTS images. Additional steps which must be taken in order to precisely coalign these images with the SERTS images were identified, but not yet implemented.

Because SERTS spectra are spatially resolvable, one can discern spectral variations with position along the slit. The spectrum within each spatial resolution element is noisier than the spatially averaged spectrum, but numerous emission lines are identifiable. For each spatial resolution element, I obtained the spectral background, subtracted it from the original spectrum, and obtained the integrated line intensities for 20 key emission lines from the background-corrected spectrum. The procedure is similar to that used for the spatially averaged spectra. In this way, densities, filling factors, temperatures, and even differential emission measure distributions can be derived as functions of position along the slit. This may provide information about certain features in active regions (like loops and sunspots), as well as about the transition from active to quiet areas. It is also extremely useful for comparison with other spatially resolved data, such as the microwave observations obtained with the VLA. It will ultimately be used, along with the microwave observations, to derive coronal magnetic fields.

The paper "Measuring Active and Quiet Sun Coronal Plasma Properties with EUV Spectra from SERTS," submitted to *The Astrophysical Journal* in April 1995, was revised but not yet resubmitted. The calibration revision has been frustrating and time consuming.

Two camera-ready conference proceedings were completed and submitted. One, for an invited talk given at the Eleventh International Colloquium on Ultraviolet and X-Ray Spectroscopy of Astrophysical and Laboratory Plasmas, is titled "Solar EUV Spectroscopy with SERTS: Measurements of Active and Quiet Sun Properties" (J. W. Brosius, J. M. Davila, R. J. Thomas, S. D. Jordan, and B. C. Monsignori-Fossi). The second, for a contributed talk given at IAU Colloquium No. 153, is titled "Measurements of Active and Quiet Sun Coronal Plasma Properties with SERTS EUV Spectra" (J. W. Brosius, J. M. Davila, R. J. Thomas, B. C. Monsignori-Fossi, and J. L. R. Saba). Both meetings were held in Japan in Spring of 1995.

3 Analysis

The problems with the laboratory calibration of the SERTS instrument were totally unexpected. I had hoped to be able to compare measured density- and temperature-insensitive line intensity ratios with their corresponding theoretical values, and find good agreement. This agreement would have supported the validity of both the laboratory measurements as well as the atomic physics calculations. The disagreement is extremely puzzling. The SERTS instrument had been flown before (in 1989), with a standard gold coated diffraction grating, and the measured line ratios agreed beautifully with their respective theoretical values. The only difference between the 1989 flight and the later flights (1991 and 1993) was the inclusion of the multilayer coated diffraction grating. Further, the laboratory measurements of the grating's response curve were clean and reproducible. They were carried out during two independent runs at NIST's SURF-II facility. At

present, the reason for the discrepancy is not known.

The problem with and the correction of the SERTS instrumental calibration underscore the value of accurate atomic physics calculations. The bottom line is that spectrographs like SERTS can be calibrated with accurately known emission line ratios. Furthermore, the ability to use emission line ratios to calibrate a spectrograph indicates the self-consistency and overall validity of relevant atomic physics parameters for numerous ions obtained from a variety of sources. Knowing this, one can confidently extract plasma parameters from the SERTS spectra as well as from SOHO/CDS spectra.

As is evident from the values listed in Table 2, active region densities typically exceed quiet Sun densities, but not necessarily by large amounts. Note that the Fe XII ion consistently yields high densities. Note also that numerous ratios are available for the Fe XIII ion. For all of the listed ratios of this ion, the 1993 active region, 1991 active region, and 1993 quiet sun yield density logarithms of 9.66 ± 0.49, 9.60 ± 0.54, and 9.03 ± 0.28, respectively. For comparison, Dere *et al.* (1979, ApJS, 40, 341) found order-of-magnitude (lower to upper limit) uncertainties on solar flare densities derived from individual line ratio measurements from Skylab data.

Filling factors were derived by combining measurements of the line intensities, calculations of the plasma densities, and the theoretical emissivities. Filling factors are listed in Table 3. A path length of $\Delta\ell = 1 \times 10^9$ cm is used. With a few exceptions, the derived filling factors are less than or comparable to unity. The numbers in curly brackets following the filling factor entries for Fe XIII give the multiplicative uncertainties associated with the range of measured density values.

Table 4 lists the temperatures derived from numerous temperature-sensitive line intensity ratios, in the isothermal approximation. The active regions are clearly hotter than the quiet sun for about half of the ratios listed in the table. However, for ratios which involve lines from only Fe XIII, XII, XI, and X, the active region and quiet sun temperatures are equal to within the derived uncertainties.

TABLE 1: Density- and Temperature-Insensitive Line Intensity Ratios

Line Ratio	Theoretical	1993 AR	1993 QS	1991 AR	1991 QS	1991 L	1989 AR
Fe XVI 360.8/335.4	0.479	0.499±0.081	0.474±0.077	0.503±0.080	0.438±0.077	0.442±0.071	0.415±0.094
Fe XV 312.6/327.0	0.581	0.793±0.200	—	1.034±0.239	—	—	0.757±0.194
Fe XV 327.0/417.3	0.341±0.094	0.217±0.038	0.395±0.104	0.324±0.058	—	0.119±0.044	0.258±0.047
Fe XV 417.3/284.1	0.0307±0.0041	0.0417±0.0069	0.0260±0.0050	0.0276±0.0046	—	0.0534±0.0124	0.0448±0.0071
Fe XV 327.0/284.1	0.0095±0.0014	0.0090±0.0015	0.0103±0.0025	0.0089±0.0015	—	0.0063±0.0021	0.0116±0.0021
Fe XV 312.6/284.1	0.0055±0.0008	0.0072±0.0018	—	0.0092±0.0020	—	—	0.0088±0.0021
Fe XV 312.6/417.3	0.183±0.040	0.172±0.043	—	0.335±0.076	—	—	0.195±0.047
Fe XIV 274.2/334.2	1.62±0.40	1.77±0.33	1.48±0.37	2.95±0.57	2.55±0.93	1.99±0.38	1.60±0.26
Fe XIII 359.8/348.2	0.259	0.199±0.036	0.215±0.059	—	0.162±0.063	0.103±0.045	0.175±0.040
Fe XIII 320.8/311.6	6.94	—	4.00±0.75	—	3.81±1.53	3.70±1.48	4.22±1.25
Fe XIII 321.5/312.2	0.475	0.296±0.070	0.485±0.116	—	—	0.510±0.148	0.383±0.102
Fe XIII 320.8/359.7	1.31±0.25	1.00±0.16	0.86±0.15	1.46±0.31	0.90±0.26	0.91±0.18	1.17±0.20
Fe XIII 312.9/359.7	0.374±0.015	0.216±0.059	0.258±0.133	—	—	0.485±0.143	0.324±0.100
Fe XIII 311.6/359.7	0.189±0.035	—	0.216±0.042	—	0.236±0.101	0.245±0.101	0.278±0.081
Fe XII 346.9/364.5	0.343±0.028	0.447±0.075	0.370±0.061	0.587±0.116	0.555±0.120	0.580±0.103	0.287±0.049
Fe XII 352.1/364.5	0.683±0.017	0.739±0.121	0.758±0.124	0.899±0.172	0.965±0.182	0.859±0.144	0.618±0.100
Fe XII 346.9/352.1	0.502±0.030	0.605±0.102	0.488±0.080	0.653±0.125	0.575±0.124	0.675±0.119	0.465±0.081
Fe XI 369.2/352.7	0.303	0.339±0.084	0.274±0.068	0.624±0.177	0.388±0.123	0.239±0.112	0.292±0.053
Fe XI 341.1/369.2	0.969±0.160	1.185±0.303	1.015±0.256	0.873±0.255	1.358±0.450	1.757±0.838	0.984±0.202
Fe XI 341.1/358.7	1.58	1.18±0.27	1.25±0.28	1.02±0.30	4.08±2.35	—	0.514±0.103
Fe X 365.6/345.7	0.420	—	0.329±0.076	—	—	—	0.567±0.107
Mg VIII 311.8/315.0	0.199	0.170±0.039	0.298±0.077	—	—	—	0.313±0.068
Mg VIII 313.7/315.0	0.385±0.009	0.292±0.057	0.287±0.059	0.292±0.079	0.436±0.092	0.820±0.192	0.317±0.062
Mg VIII 317.0/315.0	0.228±0.005	0.241±0.052	0.289±0.055	0.327±0.077	0.175±0.053	0.398±0.123	0.227±0.059
Mg VIII 339.0/315.0	0.266±0.003	0.277±0.049	0.157±0.033	0.194±0.046	0.154±0.046	—	0.213±0.042
Ni XVIII 320.6/292.0	0.46	0.379±0.103	—	0.419±0.072	—	—	0.426±0.075
Si VIII 314.4/319.8	0.352±0.010	0.378±0.083	0.509±0.091	—	0.307±0.102	0.510±0.127	0.479±0.109
Si VIII 319.8/316.2	1.50±0.02	1.32±0.26	1.38±0.26	0.76±0.20	1.59±0.32	1.29±0.30	1.27±0.24
Si IX 342.0/349.9	0.337±0.063	0.225±0.041	0.301±0.062	0.296±0.101	0.357±0.073	0.507±0.109	0.210±0.043
Si IX 349.9/345.1	1.40±0.23	1.59±0.27	1.55±0.27	1.60±0.36	1.50±0.30	1.45±0.29	1.97±0.36
Si IX 296.1/345.1	1.69±0.33	2.18±0.43	1.15±0.24	3.74±1.02	0.88±0.24	1.52±0.31	2.93±0.62
Si IX 292.8/345.1	1.10±0.07	0.572±0.204	0.987±0.293	—	—	—	0.996±0.269

TABLE 2

Density Logarithms Derived from Line Intensity Ratios

Line Ratio	1993 AR	1993 QS	1991 AR	1991 QS	1991 L	1989 AR
Fe XV 321.8/417.3	9.41 0.22	--	--	--	--	9.86 0.31
Fe XIV 353.9/334.2	9.58 0.14	9.35 0.11	9.87 0.19	9.22 0.13	9.43 0.13	9.58 0.14
Fe XII 338.3/352.1	10.30 0.12	9.96 0.11	10.42 0.15	10.24 0.14	10.19 0.13	10.36 0.14
Fe XI 308.5/369.2	9.34 0.43	9.37 0.31	--	--	9.72 0.58	<10.71
Fe XIII 320.8/348.2	9.17 0.09	8.75 0.13	9.23 0.10	8.44 0.12	8.52 0.11	9.44 0.09
Fe XIII 359.7/348.2	9.26 0.10	8.93 0.15	9.06 0.16	8.51 0.19	8.62 0.15	9.51 0.14
Fe XIII 359.7/359.8	9.44 0.13	9.04 0.22	--	8.82 0.37	9.25 0.35	<9.63
Fe XIII 311.6/348.2	--	9.14 0.11	--	8.80 0.30	8.91 0.30	10.17 0.65
Fe XIII 318.1/320.8	10.14 0.20	9.32 0.23	10.13 0.22	10.91 0.60	9.97 0.24	10.25 0.19
Fe XIII 318.1/321.5	10.07 0.20	9.16 0.10	--	--	9.34 0.15	10.11 0.23
Fe XIII 318.1/312.2	9.68 0.18	9.17 0.10	9.61 0.20	--	9.38 0.14	9.94 0.18
Fe XIII 318.1/348.2	9.36 0.09	9.01 0.03	9.42 0.10	9.15 0.07	9.04 0.03	9.73 0.14

TABLE 3

Filling factors derived from prominent emission lines of five successive ionization stages of iron, assuming $T = T_{max}$ and $\Delta\ell = 1 \times 10^9$ cm.

Line (Å)	1993 AR	1993 QS	1991 AR	1991 QS	1991 L	1989 AR
Fe XV 417.3	0.614	—	—	—	—	0.112
Fe XIV 334.2	0.395	0.127	0.0395	0.366	0.547	0.393
Fe XIII 348.2	0.146{6.0}	0.362{2.8}	0.0521{7.0}	0.0871{130}	1.01{15}	0.0447{4.6}
Fe XII 352.1	0.00738	0.00723	0.00136	0.00541	0.0163	0.00439
Fe XI 369.2	0.342	0.0659	—	—	0.0608	0.000513

Numbers in curly brackets give the multiplicative uncertainty due to the range in derived density values.

TABLE 4

Temperature Logarithms from Line Intensity Ratios Among Various Iron Ionization Stages

Line Ratio	1993 AR	1993 QS	1991 AR	1991 QS	1991 L	1989 AR
XVII 350.5/XVI 335.4	6.61±0.05	—	6.72±0.04	—	6.82±0.06	6.53±0.03
XVII 350.5/XV 284.1	6.52±0.03	—	6.59±0.02	—	6.60±0.02	6.52±0.02
XVI 335.4/XV 284.1	6.41±0.02	6.32±0.02	6.44±0.02	6.32±0.02	6.39±0.02	6.51±0.03
XVI 335.4/XIV 334.2	6.32±0.01	6.26±0.01	6.37±0.02	6.27±0.01	6.29±0.01	6.37±0.02
XVI 335.4/XIII 348.2	6.32±0.02	6.25±0.02	6.36±0.02	6.24±0.02	6.27±0.02	6.37±0.02
XVI 335.4/XII 352.1	6.29±0.01	6.24±0.01	6.32±0.01	6.23±0.01	6.25±0.01	6.32±0.01
XV 284.1/XIV 334.2	6.24±0.02	6.21±0.02	6.31±0.03	6.22±0.02	6.20±0.02	6.27±0.02
XV 284.1/XIII 348.2	6.27±0.03	6.22±0.02	6.32±0.03	6.21±0.02	6.21±0.02	6.31±0.03
XV 284.1/XII 352.1	6.25±0.01	6.21±0.01	6.28±0.01	6.20±0.01	6.21±0.01	6.27±0.01
XIV 334.2/XIII 348.2	6.31±0.04	6.22±0.03	6.32±0.04	6.19±0.03	6.22±0.03	6.37±0.04
XIV 334.2/XII 352.1	6.25±0.01	6.21±0.01	6.26±0.01	6.19±0.01	6.22±0.01	6.27±0.01
XIII 348.2/XII 352.1	6.19±0.05	6.20±0.05	6.19±0.05	6.20±0.05	6.21±0.05	6.17±0.05
XIII 348.2/XI 341.1	6.15±0.03	6.17±0.03	6.15±0.03	6.13±0.03	6.15±0.03	6.16±0.03
XIII 348.2/X 345.7	6.11±0.02	6.11±0.02	6.11±0.02	6.11±0.02	6.12±0.02	6.10±0.02
XII 352.1/XI 341.1	6.10±0.02	6.13±0.02	6.11±0.03	6.06±0.03	6.10±0.02	6.15±0.03
XII 352.1/X 345.7	6.07±0.01	6.07±0.01	6.08±0.01	6.06±0.01	6.08±0.01	6.07±0.01
XI 341.1/X 345.7	6.03±0.02	6.01±0.02	6.04±0.03	6.06±0.03	6.06±0.02	6.00±0.02

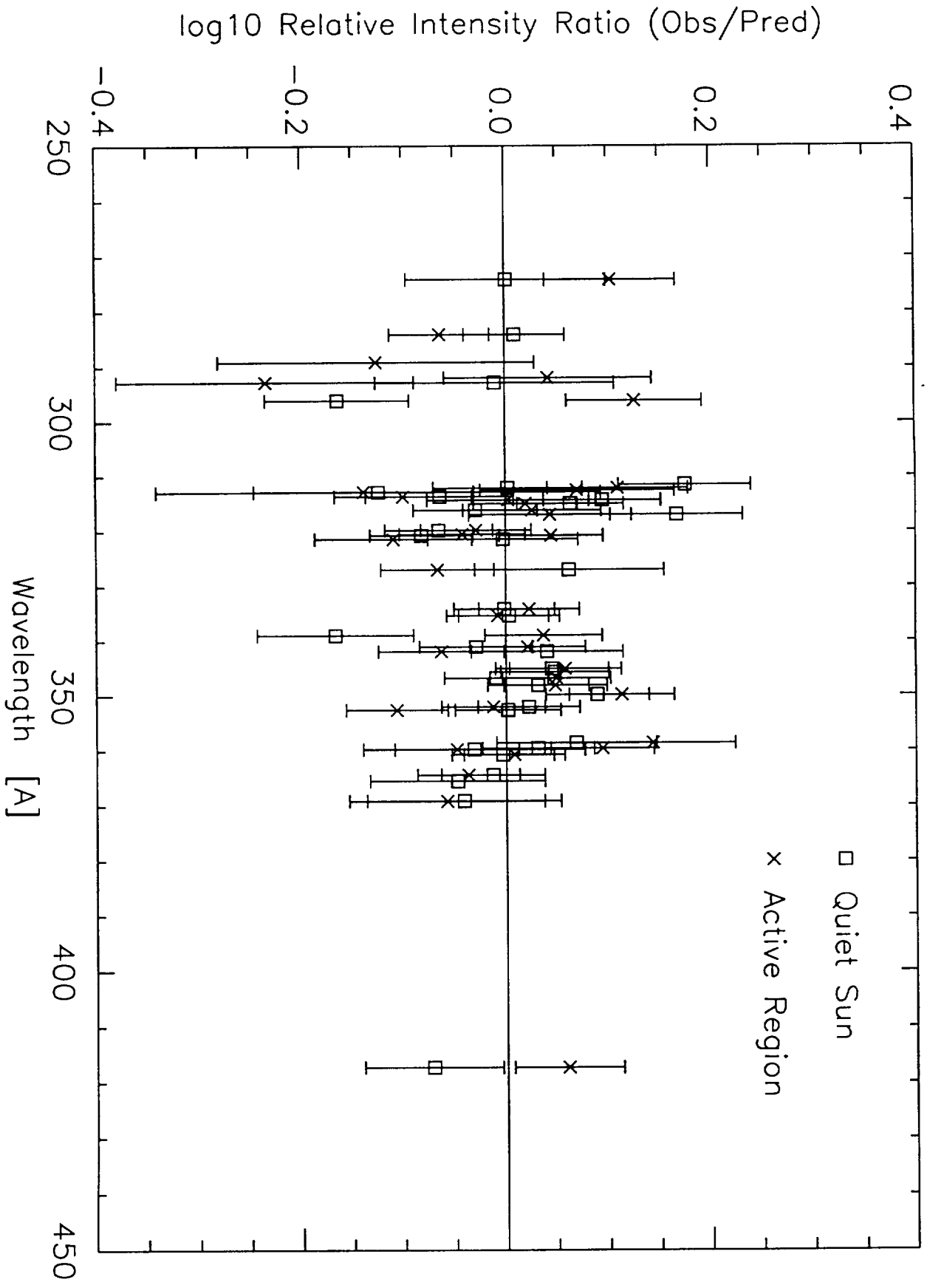
log10 Relative Intensity Ratio (Obs/Pred)
−0.4
−0.2
0.0
0.2
0.4
250
300
350
400
450
Wavelength [A]
SERTS−93 Insensitive Line Ratios
□ Quiet Sun
× Active Region

Figure 1

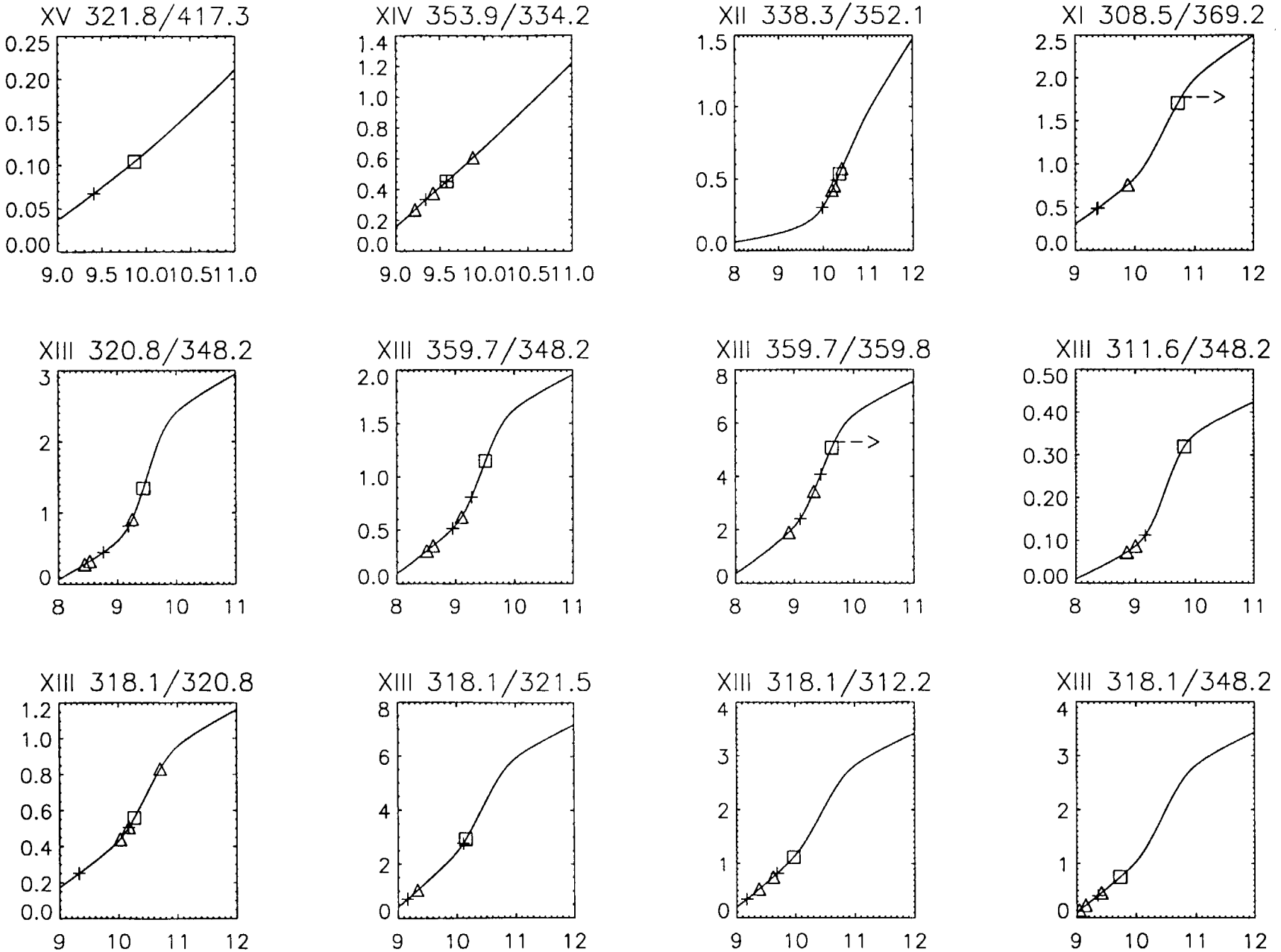
XV 321.8/417.3
XIV 353.9/334.2
XII 338.3/352.1
XI 308.5/369.2
XIII 320.8/348.2
XIII 359.7/348.2
XIII 359.7/359.8
XIII 311.6/348.2
XIII 318.1/320.8
XIII 318.1/321.5
XIII 318.1/312.2
XIII 318.1/348.2

Figure 2

NASA REPORT DOCUMENTATION PAGE (IN LIEU OF NASA FORM SF 298)

1. REPORT NO.	2. GOVERNMENT ACCESSION NO. / 3. RECIPIENT'S CATALOG NO.
4. TITLE AND SUBTITLE Plasma Properties and Magnetic Field Structure of the Solar Corona, Based on Coordinated Max '91 Observations from SERTS, the VLA, and Magnetographs	5. REPORT DATE 11 January 1996 6. PERFORMING ORGANIZATION CODE:
7. AUTHOR(S) Dr. Jeffrey W. Brosius	8. PERFORMING ORGANIZATION REPORT NO:
9. PERFORMING ORGANIZATION NAME AND ADDRESS Hughes STX Corporation 4400 Forbes Blvd. Lanham, MD 20706	10. WORK UNIT NO. 11. CONTRACT OR GRANT NO. NASW-4933
12. SPONSORING AGENCY NAME AND ADDRESS Solar Physics Branch Space Physics Division Code SS NASA Headquarters Washington, DC 20546	13. TYPE OF REPORT AND PERIOD COVERED Annual progress report for 12 July 1995 - 11 January 1996 14. SPONSORING AGENCY CODE NASA HQ/ CODE SS
15. SUPPLEMENTARY NOTES	

16. ABSTRACT

A problem was identified with the SERTS calibration as determined from laboratory measurements. The measured calibration curve yielded several density- and temperature-insensitive line intensity ratios which differed from their corresponding theoretical values, as well as a number of density-sensitive line ratios that were either too high or too low with respect to their expected theoretical ranges. A revised calibration curve was derived by requiring that the numerous available measured line intensity ratios agree with their respective theoretical values. This underscores the utility of the line ratio method for instrumental calibration verification and modification. Active region densities were found to typically exceed quiet sun densities, but not necessarily by large amounts. Active region density logarithms of 9.66 +/- 0.49 and quiet Sun density logarithms of 9.03 +/- 0.28 are obtained for the Fe XIII lines observed during the 1993 SERTS flight. Filling factors were derived by combining measurements of the line intensities, calculations of the plasma densities, and the theoretical emissivities. With a few exceptions, the derived filling factors are less than or comparable to unity. Emission line lists for each spatial resolution element were obtained along the SERTS slit. This may provide information about plasma parameters in specific active region features (loops and/or sunspots), as well as information about the transition from active to quiet areas. The paper ''Measuring Active and Quiet Sun Coronal Plasma Properties with EUV Spectra from SERTS'' was revised. Two camera-ready conference proceedings were completed and submitted. The IDL code for calculating the microwave emission from a magnetized plasma was revised, and additional necessary changes were identified. The VLA data were crudely coaligned and qualitatively compared with SERTS images.

17. KEY WORDS (SUGGESTED BY AUTHOR(S)) EUV Spectra, Corona, Microwaves, Magnetic Fields	18. DISTRIBUTION STATEMENT Space Science, Solar Physics

19. SECURITY CLASSIF. (OF THIS REPORT) None	20. SECURITY CLASSIF. (OF THIS PAGE) None	21. NO OF PAGES	22. PRICE	